

N. Danyliuk, T. Tatarchuk, A. Shyichuk

## **Estimation of Photocatalytic Degradation Rate Using Smartphone Based Analysis**

*Vasyl Stefanyk Precarpathian National University, Ivano-Frankivsk, Ukraine, e-mail: [danyliuk.nazariv@gmail.com](mailto:danyliuk.nazariv@gmail.com)*

A simple approach to test photocatalyst activity has been described. Photocatalytic degradation of a model dye was measured with using a smartphone. The color changes were registered directly in the micro-photoreactor. The model dye Rhodamine B was degraded under UV irradiation (365 nm). The effect of H<sub>2</sub>O<sub>2</sub> concentration and titanium dioxide photocatalyst dosage has been studied. Among three color systems, RGB, CIE L\*a\*b\* and HSV, the first one proved to be the most suitable for the dye determination. The reference measurements were carried out with a UV-Vis spectrophotometer. Two smartphones and two tablets with different camera resolution have been examined. The best calibration curve was obtained using Samsung Galaxy A6 smartphone with a 16 MP camera. The t-test has showed with a 95 % confidence that there are no significant differences between the dye concentrations measured with the smartphone and spectrophotometer. The values of relative standard deviation of the smartphone measurements were less than 0.5 %. Therefore, the proposed method for fast estimation of photocatalyst activity can be used in control of advanced oxidation reactions.

**Key words:** smartphone, Rhodamine B, photocatalyst, LED, photodegradation.

*Received 29 October 2020; Accepted 15 December 2020.*

### **Introduction**

The recent trend in analytical chemistry is to make the measuring techniques more feasible and wide spread. Mobile devices are increasingly used to simplify chemical analysis. Nowadays smartphone is a very common device giving access to a huge amount of information. Smartphone technology has not yet reached its evolutionary peak. Smartphones provide many opportunities to improve medical diagnostics, chemical analysis and environmental control [1]. For that reason, smartphones attract increasing attention of researchers. The confirmation is the growing number of scientific publications on smartphone-based analytical methods. The numbers of publications related to the smartphone-based and smartphone-controlled analysis are shown in Fig. 1. Probably, the number of the studies on detecting food toxins and environmental contaminants will

increase in the coming years.

For chemical analysis purposes, smartphones can be combined with paper test strips, chip-based sensors and many other detectors. For example, test strips have been combined with a smartphone to quantify bacteria in food [2]. There are various smartphone-based systems for detecting food and water contaminants, including heavy metals [3,4], microorganisms and parasites [5, 6].

The analysis of substances by a smartphone is based mainly on colorimetric [3,4], fluorescent [7], luminescent [6] and electrochemical [8] methods (Table 1). Smartphone-based assays are already used in healthcare, food control [9, 10] and environmental protection [11]. Smartphone applications [12, 13] allow detecting and quantifying many analytes. The specialized applications perform complex analytical calculations and can be used by non-professionals.

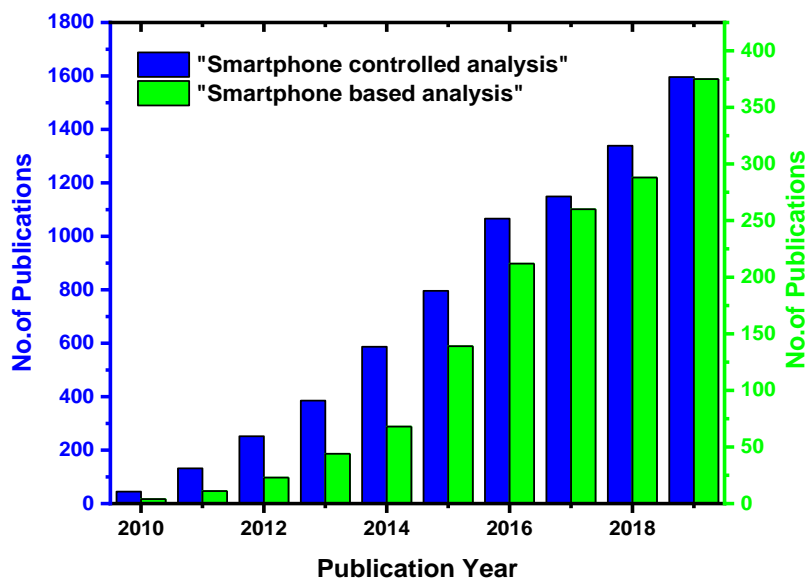


**Fig. 1.** The number of scientific publications related to the smartphone-based and the smartphone-controlled analysis for the last 10 years (according to the Scopus® database, search date: 01-10-2020).

**Table 1**

The examples of smartphone-based analysis for food and water quality control

Analysis	Detection target	Limit of detection (LOD) or linear range (LR)	Ref.
Colorimetric analysis	Fe in bioethanol fuel	LOD: 0.5 mg/ml	[4]
	Mercury ion	LOD: 50 nM	[3]
	Fluoride	LR: 0.0-2.0 mg/l	[18]
	Chlorine	LR: 0.06–2.0 ppm	[20]
	Protein	LOD: 1.0 %	[10]
	Phenol index	LOD: 2 µg/L	[26]
	Fluoride	LOD: $1.23 \times 10^{-4}$ mg/L	[19]
	Sibutramine	LOD: 1.15 µM	[24]
	Phosphate ion	LOD: 0.09 µM	[21]
	Mercury ion	LOD: 0.28 ng/mL	[22]
	Chlorine	LOD: $5.00 \times 10^{-2}$ mg/L	[23]
	Nitrite	LOD: $8.60 \times 10^{-3}$ mg/L	
	Hydrogen peroxide	LOD: 1.7 mg/L	[27]
Bioluminescence analysis	<i>P. fluorescens</i> M3A	LOD: $7.9 \times 10^6$ CFU/ml	[28]
Luminescence analysis	<i>Escherichia coli</i>	LOD: 70 CFU/ml	[6]
	<i>Staphylococcus aureus</i>	LOD: 131 CFU/ml	
Fluorescence analysis	Alkaline phosphatase	LOD: 0.078 mU/mL	[7]
	<i>Escherichia coli</i>	LOD: 5 to 10 CFU/mL	[5]
Electrochemical analysis	Hydrogen peroxide	LR: 0.0-0.429 µA L/mmol	[8]

Photometric analysis is attractive due to its simplicity [14]. Unlike fluorescence-based sensors, colorimetric sensors may work without additional light sources, so the devices are small and portable. Typically, a colorimetric method uses changes in absorbance over a given wavelengths range. The color changes are captured by the smartphone camera. Different color space systems may be used: RGB, HSV or CIE L\*a\*b\*. Colorimetric

analysis is used to detect both organic substances (dyes, toxins, formaldehyde, etc.) [15-17] and inorganic substances (fluoride [18, 19], chlorine [20], nitrite, phosphates [21], Fe [4], Cu, Pb, Hg [3, 22]). Typical objects for analysis are water [23], food [24] and drinks [25] (Table 1).

The purpose of this work is to develop a feasible method for photocatalysts testing. A smartphone

Table 2

Mobile devices used for testing		
Digital device	Model	Camera
Smartphone-1	Samsung Galaxy A6 (SM-A600FN) 3/64Gb	16 MP
Smartphone-2	Samsung Galaxy S4 mini GT-i9192	8 MP
Tablet-1	Asus ZenPad 7.0 16Gb	5 MP
Tablet-2	Huawei MediaPad T3 7 3G	2 MP

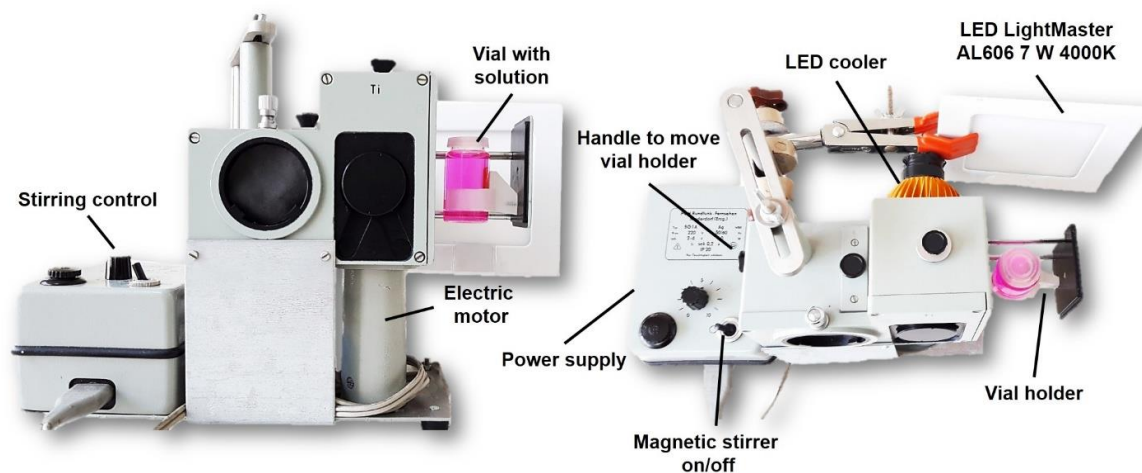


Fig. 2. General view of the micro-photoreactor.

provides fast and easy measurement of dye photodegradation rate. The exemplary photocatalyst was well-known titania Aeroxide P25 in the presence of hydrogen peroxide as a promoter. The Rhodamine B dye was as a model dye for the photodegradation. The optimal range of hydrogen peroxide concentration has been found. The photooxidation reaction was carried out in the microreactor described recently [29]. The microreactor has the following advantages: (i) small amounts of reagents and photocatalyst required; (ii) rapid replacement of the radiation source (depending on the model compound to degrade); (iii) low cost. The photooxidation rate measurements were performed using four portable devices in order to estimate a probable effect of camera parameters.

## Materials and methods

### 1.1. Photocatalyst and reagents

Titania Aeroxide P25 (Degussa/Evonik, Germany) was used as photocatalyst. This material is widely used due to its high activity in many photocatalytic reaction. The commercial P25 photocatalyst contains mixture of 70 – 80 % anatase and 20 - 30% rutile. The P25 catalyst has average BET surface area about 50 m<sup>2</sup>/g and average particle size of 30 nm [30]. The Rhodamine B (RhB) dye was obtained from Aldrich. Reagent grade hydrogen peroxide (30 %) from a local store of chemicals was diluted to 0.5 mol/L stock solution.

### 1.2. Mobile devices and spectrophotometer

The mobile devices used for testing photooxidation rate are described in Table 2.

The UV-Vis spectrophotometer ULAB 102-UV with 5 mm glass cuvettes was used for the determination of Rhodamine B concentration [29].

### 1.3. Micro-photoreactor

Front view and top view of the micro-photoreactor are shown in Fig. 2. The volume of the round glass vial is 20 mL. The UV radiation source is a 3W light-emitting diode (UV-LED) with the narrow emission range from 365 to 370 nm.

### 1.4. Dye photodegradation tests

The photodegradation experiments were carried out using 20 mL of aqueous solution of the RhB dye with the concentration of 5 mg/L. The exact mass of 30 mg of the P25 photocatalyst was added. The suspension was magnetically stirred for 20 min in the dark to reach adsorption equilibrium. The duration of the UV irradiation was 30 min. Every 5 min the vial holder was pulled out and the vial images were captured with the mobile devices (Fig. 3). Finally, the suspension was centrifuged for 10 min at 4000 rpm, and the absorbance of the supernatant was measured at 560 nm on the spectrophotometer.



Fig. 3. Color measurements using smartphone camera.

Table 3

The comparison of various approaches for RGB data analysis

Analyte	Digital device	Equation	Ref.
phosphate	scanner HP Scanjet G2710	$A = -\log\left(\frac{R}{R_0}\right)$ $[v] = \sqrt{(R - R_0)^2 + (G - G_0)^2 + (B - B_0)^2}$	[31]
Iron (II/III) in white wine	Microsoft 720p HD	$A = \log\left(\frac{B_0}{B_x}\right)$	[32]
KMnO <sub>4</sub> , CoSO <sub>4</sub> , NiSO <sub>4</sub> , CuSO <sub>4</sub>	Smartphone	$\langle I_{RGB} \rangle_{std/unknown} = \frac{R_{pixel} + G_{pixel} + B_{pixel}}{3}$ $\langle I_{RGB} \rangle_p = \log\left(\frac{\langle I_{RGB} \rangle_{blank}}{\langle I_{RGB} \rangle_{std/unknown}}\right)$	[33]
RhB dye	Smartphone	$R' = \frac{R}{R+G+B}; \quad G' = \frac{G}{R+G+B}; \quad B' = \frac{B}{R+G+B}$	This work

## II. Results and discussion

### 2.1. Calibration curves obtained with color measurements













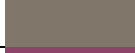











To provide reproducibility of the color measurements, a probable impact of extraneous light should be minimized. For that reason, a bright white background was used for capturing images of the vial with the colored suspensions. The used 7W LED lamp with 4000 K color temperature consists of 30 LEDs and provides flat white background. As a result of the RhB dye degradation, the reaction mixtures changed color from bright pink to pale pink and further to dirty white. The color parameters of the captured images were obtained with using the mobile application Spectrum (available on the Play Market). This application works with various color systems, such as RGB, HSV, CIE

L\*a\*b\*, CMYK, XYZ, RYB. Different approaches for analyzing raw RGB data have been reported in the literature (Table 3). We proposed new equations providing the best correlation coefficient ( $R^2$ ) in a wide range of concentrations. The normalized red component  $R'$  was calculated as the following:  $R' = \frac{R}{R+G+B}$ .

The exemplary color images captured for the TiO<sub>2</sub> suspensions with different concentrations of the RhB dye are presented in Table 4. Three color models (RGB, CIE L\*a\*b\*, HSV) were applied to describe color changes. In the RGB color system, the increase of RhB concentration leads to increase in the Red component and decrease in the Green and Blue color components. So, the Red component of the color was used for the determination of the RhB dye. In the CIE L\*a\*b\* color system, the parameters L\* and b\* do not show monotonic changes. The parameter a\* is rather increased. In the HSV color system, slight changes in the S and V parameters are

**Table 4**

The color parameters of the RhB dye solutions with different concentrations (the solution volume was 20 mL and TiO<sub>2</sub> dosage was 30 mg)

C(RhB), mg/L	Image	RGB				CIE L*a*b*			HSV		
		R	G	B	R'	L*	a*	b*	H	S	V
<b>Smartphone-1</b>											
0		172	161	155	0.352	68.5	2.9	4.5	21	9	69
1		192	122	132	0.430	58.8	28.6	6.0	351	36	75
2		206	112	130	0.460	58.3	38.9	6.8	348	45	80
3		220	112	127	0.479	60.2	43.6	11.4	351	49	86
4		207	95	107	0.506	54.6	45.4	14.9	353	54	81
5		220	96	107	0.520	56.7	49.5	18.2	354	56	86
<b>Smartphone-2</b>											
0		145	117	52	0.462	50.4	4.2	35.8	40	60	56
1		175	90	93	0.489	48.5	34.8	14.1	357	48	68
2		184	79	93	0.517	47.7	43.7	13.2	352	57	72
3		183	70	90	0.534	45.8	47.3	12.5	349	61	71
4		221	81	107	0.540	54.3	56.5	15.0	348	63	86
5		171	59	71	0.568	41.5	46.6	18.0	353	65	67
<b>Tablet-1</b>											
0		128	118	106	0.364	50.2	1.6	7.9	32	17	50
1		140	68	105	0.447	39.1	35.1	-7.3	329	51	54
2		124	35	91	0.496	30.0	43.8	-12.4	322	71	48
3		142	16	89	0.575	31.4	54.0	-8.6	325	88	55
4		155	14	66	0.660	33.2	55.6	9.4	337	90	60
5		124	12	71	0.599	26.7	48.4	-4.1	328	90	48
<b>Tablet-2</b>											
0		195	163	104	0.422	68.6	4.2	33.9	38	45	76
1		220	135	130	0.454	65.0	31.9	16.5	3	40	86
2		220	142	156	0.425	67.2	31.4	4.9	349	35	86
3		242	145	162	0.441	70.6	38.5	6.9	349	40	94
4		228	124	149	0.455	64.2	42.8	4.7	345	45	89
5		242	136	156	0.453	68.6	42.4	7.3	348	43	94

observed. Instead, the parameter H initially increases and then has a rather stable value. Thus, the calibration curves have been drawn using the parameter R' (Fig. 4). It can be seen that the calibration lines and coefficients R<sup>2</sup> are dependent on digital camera used (Fig. 4). In the first approach, better camera resolution provides larger values of the R<sup>2</sup> parameter. For example, the

Smartphone-1 with a 12MP camera provides R<sup>2</sup> = 0.996, while Tablet-2 with a 2MP camera provides R<sup>2</sup> = 0.436. The Smartphone-2 also provides rather high value R<sup>2</sup> = 0.979. Therefore, the 8MP camera is also suitable for the RhB determination. The kinetic measurements on RhB photooxidation were performed with the Smartphone-1 providing the best calibration line.

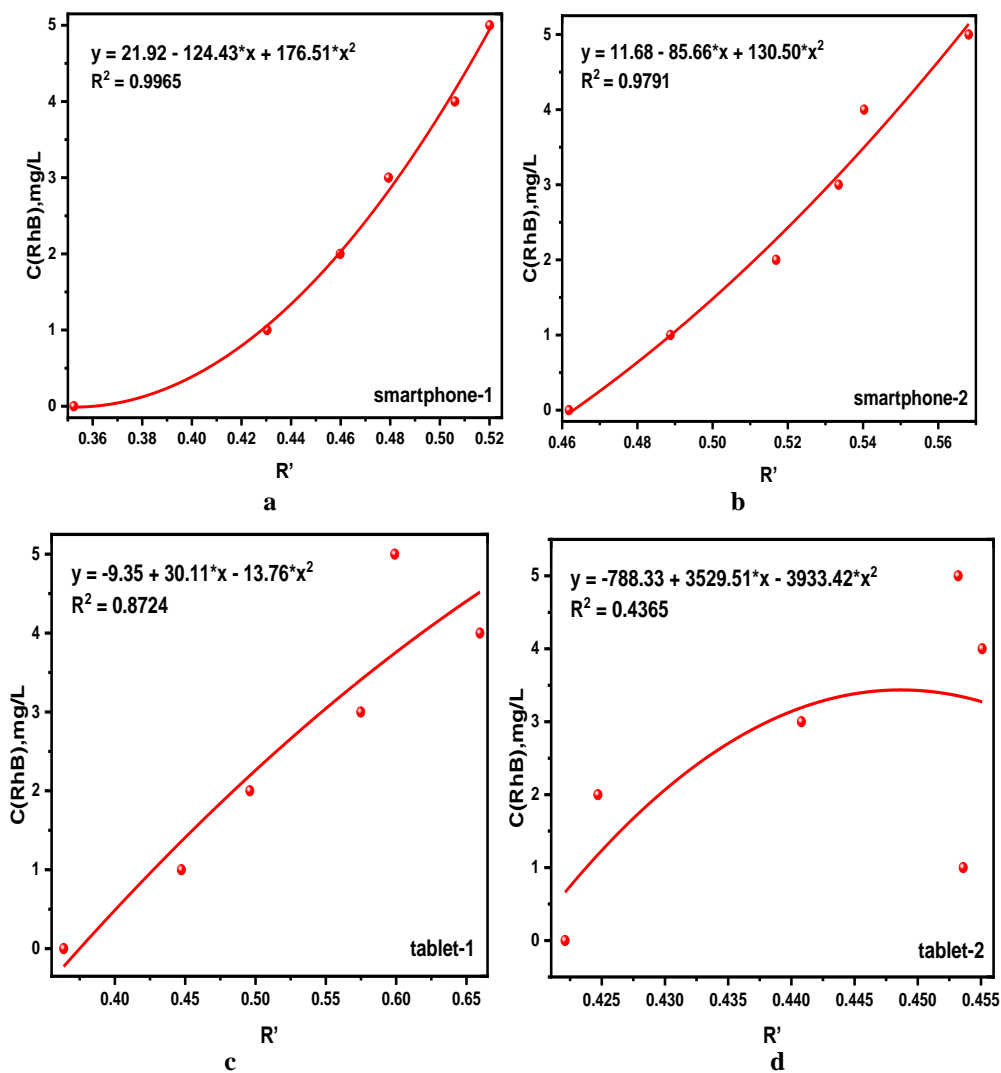
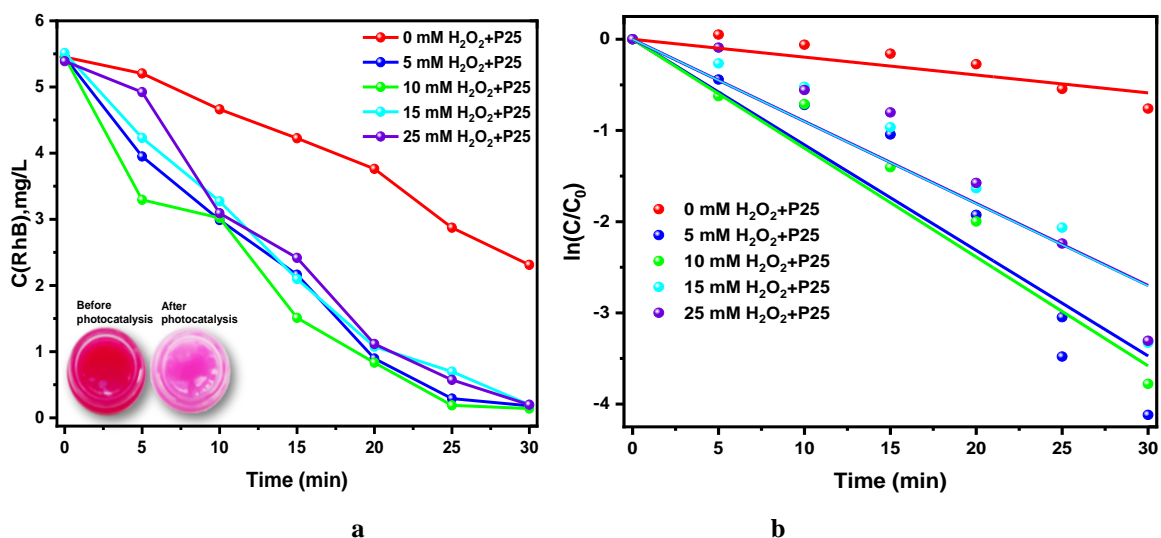


Fig. 4. Calibration curves with the normalized R' parameter.

Table 5

Color of the solutions and the values of parameter  $R' = \frac{R}{R+G+B}$  during photodegradation of the RhB dye activated with  $TiO_2$  and  $H_2O_2$ . The images were captured by Smartphone-1.

C(H <sub>2</sub> O <sub>2</sub> )	0 min	5 min	10 min	15 min	20 min	25 min	30 min
0 mM	0.520	0.524	0.5152	0.5075	0.4987	0.480	0.467
5 mM	0.5392	0.502	0.4829	0.4635	0.4243	0.394	0.386
10 mM	0.5394	0.489	0.4836	0.4454	0.4217	0.386	0.382
15 mM	0.5294	0.507	0.4889	0.4619	0.4311	0.416	0.387
25 mM	0.5274	0.519	0.4851	0.4699	0.4325	0.410	0.387



**Fig. 5.** (a) Kinetic curves of the RhB dye photodegradation; (b) transformation according the first-order kinetic model. The initial conditions were the following:  $C_0(\text{RhB}) = 5 \text{ mg/L}$ ;  $m(\text{TiO}_2) = 30 \text{ mg}$ ;  $V(\text{solution}) = 20 \text{ mL}$ ;  $C(\text{H}_2\text{O}_2) = 0 - 25 \text{ mM}$ .

**Table 6**

The parameters of the first-order kinetic model for the RhB photodegradation. The initial conditions were the same as in Fig. 5

$\text{H}_2\text{O}_2$ concentration	$k \text{ (min}^{-1}\text{)}$	$R^2$
0 mM	0.0195	0.891
5 mM	0.1157	0.959
10 mM	0.1193	0.975
15 mM	0.0901	0.959
25 mM	0.0899	0.950

## 2.2. Measurements of photocatalytic oxidation rate

The degree of photocatalyst activity depends on several parameters, such as light intensity, reactor shape, contaminant concentration, solution volume, photocatalyst dosage, pH, and others [34-39]. The final products of photocatalytic degradation of the RhB dye are water and carbon dioxide [40]. In this study, the RhB concentration has been 5 mg/L to ensure complete dye removal. The mass of  $\text{TiO}_2$  was 30 mg. Larger doses of photocatalysts could block the UV-radiation, necessary to destroy RhB [29]. The experimental images captured under the RhB photodegradation are presented in Table 5. Kinetics of the RhB photodegradation is depicted in Fig. 5a. The presence of  $\text{H}_2\text{O}_2$  leads to increase of photodegradation rate. Complete degradation of the RhB dye occurs after 30 minutes. The kinetics is rather well fitted by the first-order model. The obtained rate constants are listed in Table 6. It can be seen that the rate constant increases with increasing  $\text{H}_2\text{O}_2$  dosing, reaching a maximum at a concentration of 10 mM  $\text{H}_2\text{O}_2$ . The subsequent increase of  $\text{H}_2\text{O}_2$  concentration leads to decrease in RhB photodegradation. It can be explained by recombination of large amount of hydroxyl radicals with  $\text{H}_2\text{O}_2$  molecules.

Spectra of the final solutions were registered with the UV-Vis spectrophotometer (Fig. 6). The reliability of the

smartphone measurements was confirmed by a t-test. The t-test at 95 % confidence did not show differences between the concentrations measured by the smartphone-1 and the spectrophotometer. The data summarized in Table 7 show a good agreement between the two devices.

The mechanism of RhB photodegradation is

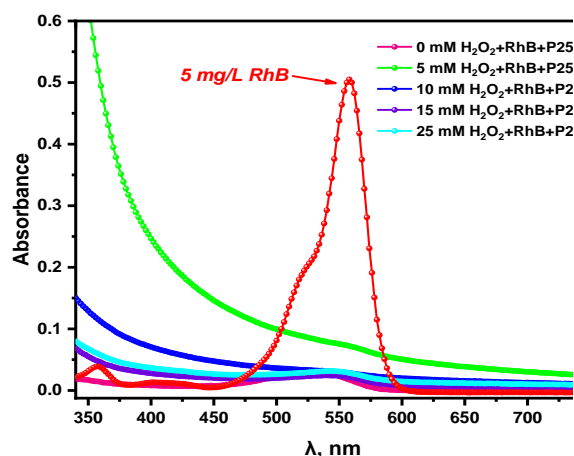


**Fig. 6.** Exemplary spectra of the RhB dye solutions after photodegradation.

Table 7

Degree of the RhB dye photodegradation (after 30 min irradiation) measured with the two devices and Relative Standard Deviation (RSD) of the smartphone measurements (n = 3).

Photodegradation degree, %		RSD, %
Spectrophotometer	Smartphone-1	
71.25	73.63	0.17
97.70	98.50	0.12
98.90	98.70	0.20
95.80	96.49	0.45
95.05	96.40	0.48

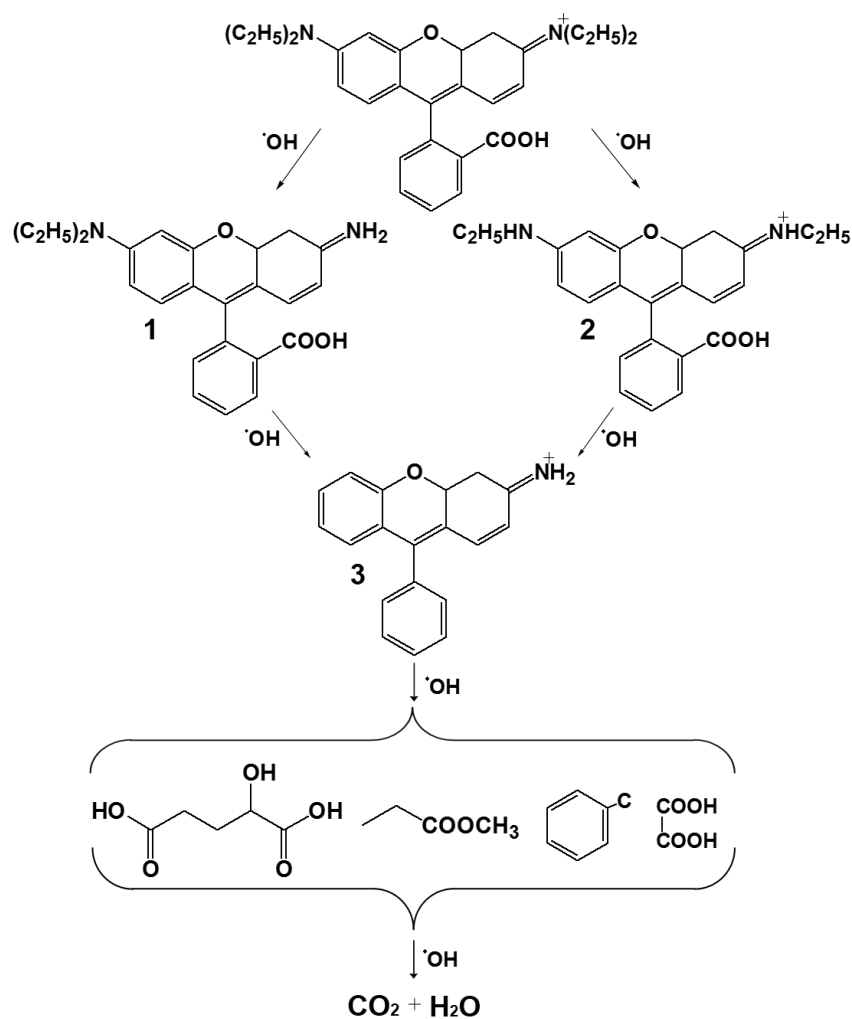


Fig. 7. The mechanism of RhB photodegradation in the presence of P25 and  $\text{H}_2\text{O}_2$ .

presented in Fig. 7. At first, auxochrome ethyl groups are detached from amino groups. As a result, the deethylated products 1-3 are formed. Second, carboxyl group is lost. The next stage is decomposition of chromophore core and formation of low molecular acidic compounds. Finally, carbon dioxide and water are formed.

## Conclusions

Currently, smartphones are well used in analytical

applications. Typically, quantitative determination is based on images recorded using a smartphone camera. In the present work, smartphone was used to study photodegradation of the RhB dye in the presence of the P25 titania photocatalyst and  $\text{H}_2\text{O}_2$ . The main advantage of this method is that the kinetic lines were registered without taking aliquots for the analysis. The microreactor uses small amount of the  $\text{TiO}_2$  photocatalyst. The Samsung Galaxy A6 smartphone showed very good repeatability in the RhB dye determination. Calibration curve for the mixtures of the RhB dye with the  $\text{TiO}_2$



catalyst were determined for the RhB concentration up to 5.0 mg/L with correlation coefficient  $R^2 = 0.996$ . The relative standard deviation ranged from 0.12 to 0.48 %. It was found that  $H_2O_2$  accelerates the dye photodegradation. However, the accelerating effect is decreased at high concentrations of  $H_2O_2$  because the formed hydroxyl radicals react with the excess of  $H_2O_2$  molecules.

#### Acknowledgements

*N. Danyliuk and T. Tatarchuk thank the Ministry of Education and Science of Ukraine for financial support in the framework of Ukrainian-Polish bilateral project "Photocatalytic hybrid systems for water purification" (0120U104158). T. Tatarchuk acknowledge Professor W.*

*Macyk (Jagellonian University, Krakow, Poland) for a productive discussion. A. Shyichuk thanks the Ministry of Education and Science of Ukraine for financial support in the framework of project no. 0120U102035.*

**Danyliuk N.** – BSc, leading specialist at the Educational and Scientific Center of Material Science and Nanotechnology;

**Tatarchuk T.** – PhD in Chemistry, Associate Professor of the Chemistry Department, Director of Educational and Scientific Center of Material Science and Nanotechnology;

**Shyichuk A.** – Doctor of Chemical Sciences, Professor of the Chemistry Department.

- [1] S. Srivastava, S. Vaddadi, S. Sadistap, *Appl. Water Sci.* 8 (2018) (doi:10.1007/s13201-018-0780-0).
- [2] H. Liu, F. Zhan, F. Liu, M. Zhu, X. Zhou, D. Xing, *Biosens. Bioelectron.* 62, 38 (2014) (doi:10.1016/j.bios.2014.06.020).
- [3] G.H. Chen, W.Y. Chen, Y.C. Yen, C.W. Wang, H.T. Chang, C.F. Chen, *Anal. Chem.* 86, 6843 (2014) (doi:10.1021/ac5008688).
- [4] A.F. João, A.L. Squizzato, G.M. Fernandes, R.M. Cardoso, A.D. Batista, R.A.A. Muñoz, *Microchem. J.* 146, 1134 (2019) (doi:10.1016/J.MICROC.2019.02.053).
- [5] H. Zhu, U. Sikora, A. Ozcan, *Analyst.* 137, 2541 (2012) (doi:10.1039/c2an35071h).
- [6] A. Irhas Robby, S. Gi Kim, U. Han Lee, I. In, G. Lee, S. Young Park, *Chem. Eng. J.* 126351 (2020) (doi:10.1016/j.cej.2020.126351).
- [7] L. Hou, Y. Qin, J. Li, S. Qin, Y. Huang, T. Lin, L. Guo, F. Ye, S. Zhao, *Biosens. Bioelectron.* 143, 111605 (2019) (doi:10.1016/j.bios.2019.111605).
- [8] J.T.C. Barragan, L.T. Kubota, *Electrochim. Acta.* 341, 136048 (2020) (doi:10.1016/j.electacta.2020.136048).
- [9] P.S. Liang, T.S. Park, J.Y. Yoon, *Sci. Rep.* 4, 4 (2014) (doi:10.1038/srep05953).
- [10] A.F.S. Silva, F.R.P. Rocha, *Food Control.* 115, 107299 (2020) (doi:10.1016/j.foodcont.2020.107299).
- [11] G.K. Özdemir, A. Bayram, V. Kiliç, N. Horzum, M.E. Solmaz, *Anal. Methods* 9, 579 (2017) (doi:10.1039/c6ay03073d).
- [12] M. Trojanowicz, *Instrumental Innovations and* 5, 2 (2017) (doi:10.4172/2329-6798.1000).
- [13] S. Álvaro, G. Marín, S. Vincent, Á.G. Marín, W. Van Hoeve, P. García-sánchez, N. Convine, A. Rosser-james, M. Tyler, K. Bando, L. Warncke, A. Lee, V. Vogel, *Lab Chip.* 15 4491 (2013) (doi:10.1039/c2lc41193h).
- [14] R.H. Tang, H. Yang, J.R. Choi, Y. Gong, S.S. Feng, B. Pingguan-Murphy, Q.S. Huang, J.L. Shi, Q.B. Mei, F. Xu, *Crit. Rev. Biotechnol.* 37 411 (2017) (doi:10.3109/07388551.2016.1164664).
- [15] T. Tatarchuk, M. Naushad, J. Tomaszewska, P. Kosobucki, M. Myslin, H. Vasylyeva, P. Ścigalski, *Environ. Sci. Pollut. Res.* 27 26681 (2020) (doi:10.1007/s11356-020-09043-1).
- [16] P. Taylor, M. Naushad, A. Mittal, M. Rathore, V. Gupta, *Sensors* 14, 37 (2014) (doi:10.1080/19443994.2014.904823).
- [17] M. Naushad, *Chem. Eng. J.* 235, 100 (2014) (doi:10.1016/j.cej.2013.09.013).
- [18] S. Levin, S. Krishnan, S. Rajkumar, N. Halery, P. Balkunde, *Sci. Total Environ.* 551-552, 101 (2016) (doi:10.1016/j.scitotenv.2016.01.156).
- [19] I. Hussain, K.U. Ahamad, P. Nath, *Anal. Chem.* 89, 767 (2017) (doi:10.1021/acs.analchem.6b03424).
- [20] S. Sumriddetchajorn, K. Chaitavon, Y. Intaravanne, *Sensors Actuators B Chem.* 191, 561 (2014) (doi:10.1016/J.SNB.2013.10.024).
- [21] X. Li, B. Liu, Z. Hu, P. Liu, K. Ye, J. Pan, X. Niu, *Environ. Res.* 189, 109921 (2020) (doi:10.1016/j.envres.2020.109921).
- [22] W. Xiao, M. Xiao, Q. Fu, S. Yu, H. Shen, H. Bian, Y. Tang, *Sensors (Switzerland)* 16, (2016) (doi:10.3390/s16111871).
- [23] M. Sargazi, M. Kaykhaii, *Spectrochim. Acta - Part A Mol. Biomol. Spectrosc.* 227, 117672 (2020) (doi:10.1016/j.saa.2019.117672).
- [24] K. Chaisiwamongkhon, S. Labadae, S. Pon-in, S. Pinsrithong, T. Bunchuay, A. Phonchai, *Microchem. J.* 158, 105273 (2020) (doi:10.1016/j.microc.2020.105273).
- [25] J.R. Choi, Z. Liu, J. Hu, R. Tang, Y. Gong, S. Feng, H. Ren, T. Wen, H. Yang, Z. Qu, B. Pingguan-Murphy, F. Xu, *Anal. Chem.* 88, 6254 (2016) (doi:10.1021/acs.analchem.6b00195).
- [26] A. Shahvar, M. Saraji, D. Shamsaei, *Microchem. J.* 154, 104611 (2020) (doi:10.1016/j.microc.2020.104611).
- [27] M.J.A. Lima, M.K. Sasaki, O.R. Marinho, T.A. Freitas, R.C. Faria, B.F. Reis, F.R.P. Rocha, *Microchem. J.* 157, 105042 (2020) (doi:10.1016/j.microc.2020.105042).

- [28] H. Kim, Y. Jung, I.J. Doh, R.A. Lozano-Mahecha, B. Applegate, E. Bae, *Sci. Rep.* 7, 1 (2017) (doi:10.1038/srep40203).
- [29] N.V. Danyliuk, T.R. Tatarchuk, A.V. Shyichuk, *Phys. Chem. Solid State.* 2, 338 (2020) (doi:https://doi.org/10.15330/pcss.21.2.338-346).
- [30] Z. Shayegan, C.S. Lee, F. Haghghat, *J. Environ. Chem. Eng.* 7, 103390 (2019) (doi:10.1016/j.jece.2019.103390).
- [31] H. Colzani, Q.E.A.G. Rodrigues, C. Fogaça, J.L.N. Gelinski, E.R. Pereira-Filho, E.M. Borges, Um exemplo didático para ensino de química, 40, 833 (2017) (doi:10.21577/0100-4042.20170035).
- [32] J.H. Santos Neto, I.S.A. Porto, M.P. Schneider, A.M.P. dos Santos, A.A. Gomes, S.L.C. Ferreira, *Talanta.* 194, 86 (2019) (doi:10.1016/j.TALANTA.2018.09.102).
- [33] S. Šafranko, P. Živković, A. Stanković, M. Medvidović-Kosanović, A. Széchenyi, S. Jokić, *J. Chem. Educ.* 96, 1928 (2019) (doi:10.1021/acs.jchemed.8b00920).
- [34] I.F. Mironyuk, L.M. Soltys, T.R. Tatarchuk, V.I. Tsinurchyn, *WPhys. Chem. Solid State* 21, 300 (2020) (doi:https://doi.org/10.15330/pcss.21.2.300-311).
- [35] T. Tatarchuk, A. Peter, B. Al-Najar, J. Vijaya, M. Bououdina, Photocatalysis: Activity of Nanomaterials, in: C.M. Hussain, A.K. Mishra (Eds.), *Nanotechnol. Environ. Sci.*, (Wiley-VCH Verlag GmbH & Co. KGaA, Germany, Weinheim, 2018). (doi:10.1002/9783527808854.ch8).
- [36] R. Chen, X. Zhang, H. Liu, X. Song, Y. Wei, *RSC Adv.* 5, 76548 (2015) (doi:10.1039/c5ra13586a).
- [37] Q. Wang, J. Lian, Q. Ma, Y. Bai, J. Tong, J. Zhong, R. Wang, H. Huang, B. Su, *New J. Chem.* 39, 7112 (2015) (doi:10.1039/c5nj00987a).
- [38] L. Zou, X. Shen, Q. Wang, Z. Wang, X. Yang, M. Jing, *J. Mater. Res.* 30, 2763 (2015) doi:10.1557/jmr.2015.263.
- [39] A. Alshammari, A. Bagabas, M. Assulami, *Arab. J. Chem.* 12, 1406 (2019) (doi:10.1016/j.arabjc.2014.11.013).
- [40] N. Guo, H. Liu, Y. Fu, J. Hu, *Optik (Stuttg)* 201, 163537 (2019) (doi:10.1016/j.ijleo.2019.163537).

Н. Данилюк, Т. Татарчук, О. Шийчук

## Оцінка швидкості фотокаталітичної деградації за допомогою смартфона

ДВНЗ «Прикарпатський національний університет імені Василя Стефаника», Івано-Франківськ, Україна,  
e-mail: [danyliuk.nazariy@gmail.com](mailto:danyliuk.nazariy@gmail.com)

Представлено простий метод перевірки активності фотокаталізатора. Фотокаталітичну деградацію модельного барвника вимірювали за допомогою смартфона. Зміни кольору реєстрували безпосередньо в мікрофотореакторі. Модельний барвник Родамін В розкладався під дією ультрафіолетового опромінення (365 нм). Досліджено вплив концентрації  $\text{H}_2\text{O}_2$  та маси фотокаталізатора діоксиду титану на фотокаталітичну деградацію родаміну В. Серед трьох колірних систем, RGB, CIE  $L^*a^*b^*$  та HSV, перша виявилася найбільш придатною для визначення барвника. Контрольні вимірювання проводили за допомогою UV-Vis спектрофотометра. Випробувано два смартфони та два планшети з різною роздільною здатністю камери. Найкраща калібрувальна крива була отримана за допомогою смартфона Samsung Galaxy A6 з 16-мегапіксельною камерою. Встановлено, що між концентраціями виміряними смартфоном та спектрофотометром, немає суттєвих відмінностей. Значення відносного середньоквадратичного відхилення вимірювань на смартфоні становить менше 0,5 %. Отже, запропонований метод швидкої оцінки активності фотокаталізатора може бути використаний для контролю реакцій фотоокислення.

**Ключові слова:** смартфон, родамін В, фотокаталізатор, світлодіод, фотодеградація.